The EMBO Journal Vol.17 No.22 pp.6633–6648, 1998

Targeted downregulation of caveolin-1 is sufficient to drive cell transformation and hyperactivate the p42/44 MAP kinase cascade

Ferruccio Galbiati[1], Daniela Volonté[1], Jeffrey A.Engelman[1], Genichi Watanabe[2], Robert Burk[3], Richard G.Pestell[2] and Michael P.Lisanti[1,5]

The Albert Einstein Cancer Center, [1]Department of Molecular Pharmacology, [2]Departments of Developmental and Molecular Biology and Medicine, and [3]Departments of Pediatrics, Microbiology and Immunology, and Epidemiology and Social Medicine, Albert Einstein College of Medicine, 1300 Morris Park Avenue, Bronx, NY 10461, USA

[5]Corresponding author
e-mail: lisanti@aecom.yu.edu

Caveolin-1 is a principal component of caveolae membranes *in vivo*. Caveolin-1 mRNA and protein expression are lost or reduced during cell transformation by activated oncogenes. Interestingly, the human caveolin-1 gene is localized to a suspected tumor suppressor locus (7q31.1). However, it remains unknown whether downregulation of caveolin-1 is sufficient to mediate cell transformation or tumorigenicity. Here, we employ an antisense approach to derive stable NIH 3T3 cell lines that express dramatically reduced levels of caveolin-1 but contain normal amounts of caveolin-2. NIH 3T3 cells harboring antisense caveolin-1 exhibit anchorage-independent growth, form tumors in immunodeficient mice and show hyperactivation of the p42/44 MAP kinase cascade. Importantly, transformation induced by caveolin-1 downregulation is reversed when caveolin-1 protein levels are restored to normal by loss of the caveolin-1 antisense vector. In addition, we show that in normal NIH 3T3 cells, caveolin-1 expression levels are tightly regulated by specific growth factor stimuli and cell density. Our results suggest that upregulation of caveolin-1 may be important in mediating contact inhibition and negatively regulating the activation state of the p42/44 MAP kinase cascade.

Keywords: caveolae/caveolin-1/contact inhibition/Ras-p42/44 MAP kinase cascade/tumor suppressor activity

Introduction

Caveolae are 50–100 nm vesicular invaginations of the plasma membrane (Severs, 1988). It has been proposed that caveolae participate in vesicular trafficking events and signal transduction processes (Lisanti *et al*., 1994a; Couet *et al*., 1997a; Okamoto *et al*., 1998). Caveolin, a 21–24 kDa integral membrane protein, is a principal component of caveolae membranes *in vivo* (Glenney, 1989, 1992; Glenney and Soppet, 1992; Kurzchalia *et al*., 1992; Rothberg *et al*., 1992).

Caveolin is only the first member of a new gene family; as a consequence, caveolin has been re-termed caveolin-1 (Scherer *et al*., 1996). Caveolin-2 shows the same tissue distribution as caveolin-1 (Scherer *et al*., 1997), while caveolin-3 is only expressed in striated muscle cell types (cardiac and skeletal) (Way and Parton, 1995; Song *et al*., 1996b; Tang *et al*., 1996). It has been proposed that caveolin family members function as scaffolding proteins (Sargiacomo *et al*., 1995) to organize and concentrate specific lipids (cholesterol and glyco-sphingolipids; Fra *et al*., 1995a; Murata *et al*., 1995; Li *et al*., 1996b) and lipid-modified signaling molecules (Src-like kinases, H-Ras, eNOS and G-proteins; Li *et al*., 1995, 1996a,b; Garcia-Cardena *et al*., 1996; Shaul *et al*., 1996; Song *et al*., 1996a) within caveolae membranes. In support of this idea, caveolin-1 binding can functionally suppress the GTPase activity of hetero-trimeric G-proteins and inhibit the kinase activity of Src-family tyrosine kinases through a common caveolin domain, termed the caveolin-scaffolding domain (Li *et al*., 1995, 1996a; Song *et al*., 1996a).

Since the identification of the caveolin-scaffolding domain and caveolin-binding sequence motifs, these observations have been extended to other caveolin-interacting proteins. Functional caveolin-binding motifs have been deduced in both tyrosine and serine/threonine kinases, as well as eNOS (Li *et al*., 1996a; Couet *et al*., 1997c; Garcia-Cardena *et al*., 1997; Ju *et al*., 1997; Michel *et al*., 1997; Oka *et al*., 1997; Engelman *et al*., 1998b). In all cases examined, the caveolin-binding motif is located within the enzymatically active catalytic domain of a given signaling molecule. For example, in the case of tyrosine and serine/threonine kinases, a kinase domain consists of 11 conserved subdomains (I–XI) (Couet *et al*., 1997c; Oka *et al*., 1997; Engelman *et al*., 1998b). The caveolin-binding motif is located within conserved kinase subdomain number IX, suggesting that caveolin could function as a 'general kinase inhibitor' (Okamoto *et al*., 1998). This hypothesis has been substantiated by the observation that the caveolin scaffolding domain inhibits Src family tyrosine kinases (c-Src/Fyn), EGF-R, Neu and PKC with similar potencies (Li *et al*., 1996a; Couet *et al*., 1997c; Oka *et al*., 1997; Engelman *et al*., 1998b).

Sessa and colleagues have performed site-directed mutagenesis to modify the predicted caveolin-binding motif (from FSAAPFSGW to ASAAPASGA) within eNOS (Garcia-Cardena *et al*., 1997). It is known from *in vitro* studies that aromatic residues (W, F or Y) are required for the proper recognition of the caveolin-binding motif (Couet *et al*., 1997b). In their work, they show that mutation of the caveolin-binding motif within eNOS blocks the ability of caveolin-1 to inhibit eNOS activity *in vivo* (Garcia-Cardena *et al*., 1997). These findings provide the first demonstration that a caveolin-binding motif is relevant and functional *in vivo*.

The direct interaction of caveolin with signaling molecules leads to their inactivation (Lisanti *et al*., 1994a; Couet *et al*., 1997a; Okamoto *et al*., 1998). Since many of these signaling molecules can cause cellular transformation when constitutively activated, it is reasonable to speculate that caveolin itself may possess transformation suppressor activity. Consistent with this hypothesis, both caveolae and caveolin are most abundantly expressed in terminally differentiated cells: adipocytes, endothelial cells and muscle cells (Bretscher and Whytock, 1977; Forbes *et al*., 1979; Fan *et al*., 1983; Simionescu and Simionsecu, 1983; Scherer *et al*., 1994, 1996). In addition, caveolin-1 mRNA and protein expression are lost or reduced during cell transformation by activated oncogenes such as v-abl and H-ras (G12V); caveolae are absent from these cell lines (Koleske *et al*., 1995).

The potential 'transformation suppressor' activity of caveolin-1 has recently been evaluated by using an inducible expression system to upregulate caveolin-1 expression in oncogenically transformed cells. Induction of caveolin-1 expression in v-Abl- and H-Ras (G12V)-transformed NIH 3T3 cells abrogated the anchorage-independent growth of these cells in soft agar and resulted in the *de novo* formation of caveolae (Engelman *et al*., 1997). Thus, downregulation of caveolin-1 expression and caveolae organelles may be critical for maintaining the transformed phenotype. However, it remains unknown whether a loss of caveolin-1 protein expression is sufficient to mediate cell transformation.

Caveolae have also been implicated in signaling through the p42/44 MAP kinase pathway. Morphological studies have directly shown that ERK-1/2 is concentrated in plasma membrane caveolae *in vivo* using immunoelectron microscopy (Liu *et al*., 1997b). Evidence has been presented suggesting that other components of the p42/44 MAP kinase cascade are localized within caveolae membranes. These include receptor tyrosine kinases (EGF-R; PDGF-R; Ins-R) (Smart *et al*., 1995; Liu *et al*., 1996; Mineo *et al*., 1996; Liu *et al*., 1997a), H-Ras (Mineo *et al*., 1996; Song *et al*., 1996a), Raf kinase (Mineo *et al*., 1996), 14-3-3 proteins (Liu *et al*., 1996), ERK (Lisanti *et al*., 1994b; Liu *et al*., 1996), Shc (Liu *et al*., 1996), Grb-2 (Liu *et al*., 1996), mSos-1 (Liu *et al*., 1996) and Nck (Liu *et al*., 1996).

Recently, we examined the functional role of caveolins in regulating signaling along the MAP kinase cascade (Engelman *et al*., 1998a). Co-expression with caveolin-1 dramatically inhibited signaling from EGF-R, Raf, MEK-1 and ERK-2 to the nucleus *in vivo* (Engelman *et al*., 1998a). Using a variety of caveolin-1 deletion mutants, we mapped this *in vivo* inhibitory activity to caveolin-1 residues 32–95. In addition, peptides derived from this region of caveolin-1 (i.e. the caveolin-scaffolding domain) also inhibited the *in vitro* kinase activity of purified MEK-1 and ERK-2 (Engelman *et al*., 1998a). Thus, caveolin-1 can inhibit signal transduction from the p42/44 MAP kinase cascade both *in vitro* and *in vivo* by acting as a natural endogenous inhibitor of both MEK and ERK. Conversely, a prediction of these findings would be that downregulation of caveolin-1 should lead to constitutive activation of the p42/44 MAP kinase pathway. As constitutive activation of the p42/44 MAP kinase cascade is sufficient to mediate cell transformation, another predicted consequence of caveolin-1 downregulation would be cell transformation.

In order to test this hypothesis directly, we have employed an antisense approach to derive stable NIH 3T3 cell lines that express dramatically reduced levels of caveolin-1, but contain normal amounts of caveolin-2. Here, we show that antisense mediated reductions in caveolin-1 protein expression are sufficient to drive oncogenic transformation and constitutively activate the p42/44 MAP kinase cascade. In normal NIH 3T3 cells, we find that caveolin-1 expression levels are downregulated in rapidly dividing cells and dramatically upregulated at confluency. Our results suggest that upregulation of caveolin-1 expression levels may be important in mediating normal contact inhibition and in negatively regulating the activation state of the p42/44 MAP kinase cascade. This is the first demonstration that a loss of caveolin-1 expression is sufficient to mediate cellular transformation. In accordance with our current findings, we have recently localized the caveolin-1 gene to a suspected tumor suppressor locus in mice (6-A2) and humans (7q31) that is deleted in many forms of cancer (Engelman *et al*., 1998c,d).

Results

Targeted downregulation of caveolin-1 protein expression, but not caveolin-2, in NIH 3T3 cells harboring caveolin-1 antisense

In order to selectively downregulate the expression of the caveolin-1 protein, we engineered two different expression vectors containing the full-length untagged murine caveolin-1 cDNA in the antisense orientation. These antisense constructs were first tested in transient transfection assays with Cos-7 cells and were found to significantly reduce the expression levels of the endogenous caveolin-1 protein, as compared with mock-transfected controls (not shown).

Given the partial success of this approach in transient transfections, we decided to derive stable cell lines that harbor these caveolin-1 antisense constructs. For this purpose, we used the well-established murine NIH 3T3 cell line. These cells contain caveolae and express caveolins 1 and 2, as we have shown previously (Koleske *et al*., 1995; Engelman *et al*., 1997; Scherer *et al*., 1997). In addition, NIH 3T3 cells have been used by many investigators as a model system to study the tumorigenicity of a given activated oncogene.

Figure 1A shows a Western blot analysis of the expression of caveolin-1 in Ras-transformed NIH 3T3 cells, parental NIH 3T3 cells and three independent NIH 3T3 clones harboring caveolin-1 antisense vector (termed A1, 25 and M). Note that caveolin-1 levels are effectively reduced in all three antisense clones tested. In addition, these three clones were derived using two independent vectors. Clones A1 and M were derived using pCAGGS (hygromycin resistance) and clone 25 was derived using pCB6 (G418 resistance) (see Materials and methods). Importantly, expression of caveolin-1 is reduced ~15- to 20-fold, but is not eliminated. Two exposures are shown to better illustrate this point. In addition, caveolin-2 levels were not affected by the expression of caveolin-1 antisense, demonstrating that the expression of caveolin-1 antisense selectively downregulates the expression of the caveolin-1

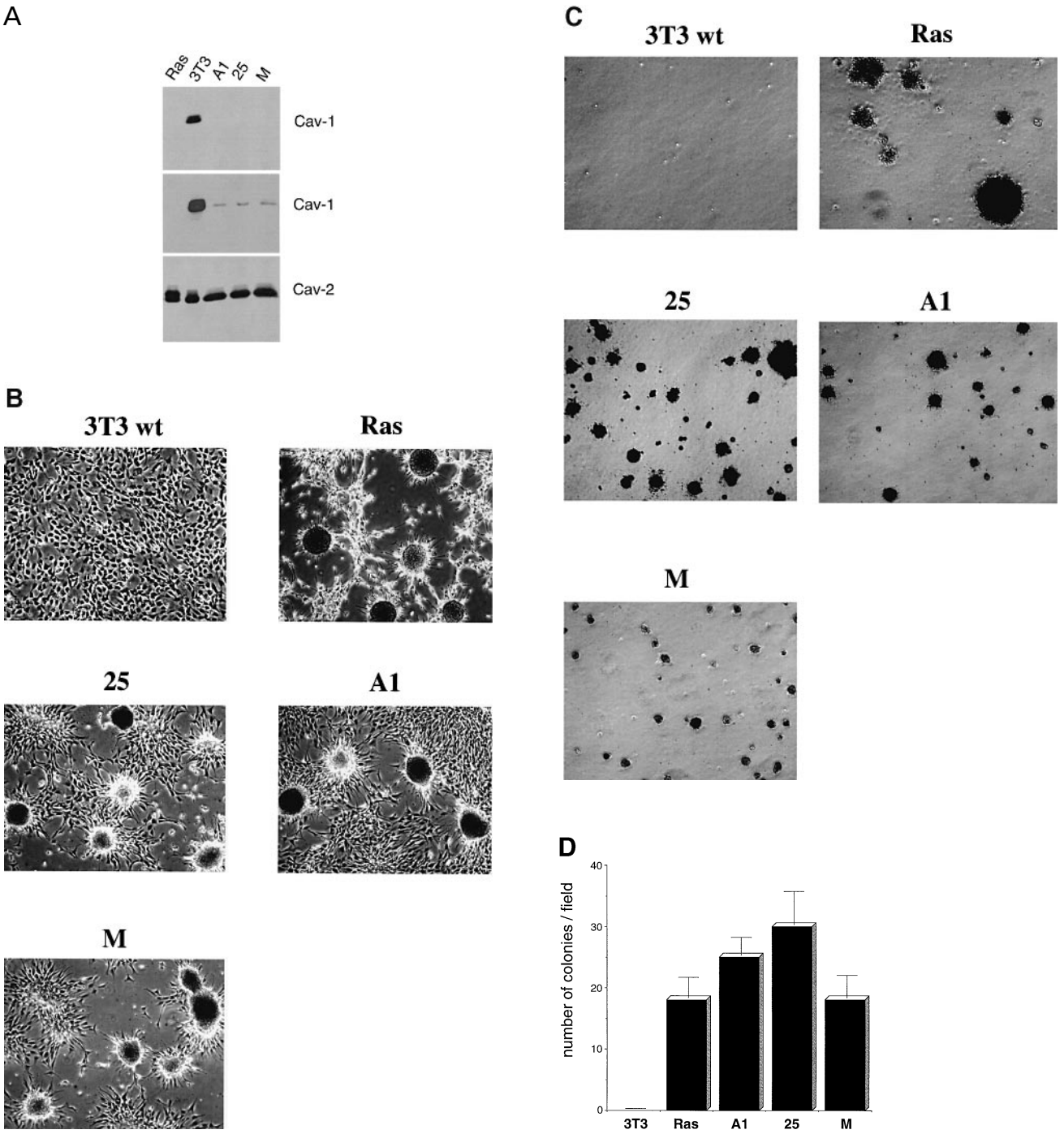

Fig. 1. Derivation of NIH 3T3 cells harboring caveolin-1 antisense. (**A**) Western blot analysis. Expression of caveolins 1 and 2 in normal NIH 3T3 cells and in NIH 3T3 cells harboring caveolin-1 antisense. Lysates were prepared from parental NIH 3T3 cells, Ras-transformed NIH 3T3 cells, and NIH 3T3 cells lines harboring antisense caveolin-1 (termed A1, 25, and M). After SDS–PAGE and transfer to nitrocellulose, immunoblotting was performed with mono-specific antibody probes that recognize only caveolin-1 (mAb 2297) or caveolin-2 (mAb 65). Note that only reductions in caveolin-1 protein expression were observed, while levels of caveolin-2 remain relatively constant in all the cell lines examined. Upper panel, caveolin-1 immunoblot; middle panel, caveolin-1 immunoblot (a longer exposure to show residual levels of caveolin-1); and lower panel, caveolin-2 immunoblot. Each lane contains equal amounts of total protein. (B–D) Morphological characterization. NIH 3T3 cells harboring caveolin-1 antisense spontaneously form foci in Petri dishes and show anchorage-independent growth in soft agar. Parental NIH 3T3 cells, Ras-transformed NIH 3T3 cells and NIH 3T3 cells lines harboring antisense caveolin-1 (termed A1, 2 5, and M) were compared for their ability to generate foci or to undergo anchorage-independent growth in soft agar. (**B**) Foci formation in plastic tissue culture dishes. (**C**) Growth and colony formation in soft agar. (**D**) Quantitation of growth in soft agar is shown. The number of colonies per field is as indicated. Note that the behavior of NIH 3T3 cells lines harboring antisense caveolin-1 is closest to that of Ras-transformed NIH 3T3 cells under these conditions.

protein. NIH 3T3 cells harboring vector alone did not show any changes in the expression of caveolin-1.

As expected, caveolae were also downregulated in these caveolin-1 antisense cell lines, as seen by transmission electron microscopy (data not shown). In support of this observation, we and others have previously shown that expression of caveolin-1, but not caveolin-2, is sufficient to drive the formation of caveolae or caveolae-like vesicles

in heterologous expression systems (Fra *et al*., 1995b; Scherer *et al*., 1995; Engelman *et al*., 1997; Scherer *et al*., 1997; Li *et al*., 1998).

NIH 3T3 cells harboring caveolin-1 antisense show a loss of contact inhibition and anchorage-independent growth, and appear morphologically transformed

To investigate whether targeted downregulation of the caveolin-1 protein is sufficient to drive cell transformation, we next subjected these cell lines to assays that are routinely used to measure oncogenic potential. All three NIH 3T3 cell clones harboring caveolin-1 antisense spontaneously formed foci in Petri dishes and exhibited growth in soft agar (Figure 1B–D). Ras-transformed NIH 3T3 cells served as a positive control and parental NIH 3T3 cells served as a negative control for these assays; quantitation of these results is presented in Figure 1D. In addition, NIH 3T3 cells harboring vector alone did not show foci formation or growth in soft agar (see below). These results suggest that targeted downregulation of caveolin-1 protein expression disrupts contact inhibition and leads to anchorage-independent growth.

Closer examination of NIH 3T3 cells harboring caveolin-1 antisense by scanning electron microscopy reveals that these cells also have a dramatically altered morphology (Figure 2). They contain an increased number of fine projections and lamellopodia, and exhibit a loss of contact inhibition, as compared with normal NIH 3T3 cell controls.

NIH 3T3 cells harboring caveolin-1 antisense are tumorigenic in immunodeficient strains of mice

As NIH 3T3 cells harboring caveolin-1 antisense behaved as expected for a transformed cell line, we next assessed their ability to form tumors in immuno-deficient strains of mice (Figure 3). All three cell lines were tumorigenic in this assay system, forming tumors with high frequency (65–100%). After 2–3 weeks, these tumors reached masses of ~2–4 g. Importantly, no tumors were observed with normal NIH 3T3 cells used for control injections. These results indicate that downregulation of caveolin-1 protein expression is sufficient to confer tumorigenicity.

Activation of the p42/44 MAP kinase pathway, but not the p38 MAP kinase pathway, in NIH 3T3 cells harboring caveolin-1 antisense

What is the mechanism by which downregulation of caveolin-1 promotes a loss of contact inhibition, anchorage-independent growth and tumorigenicity? One possibility is through the de-repression of signal transduction, as caveolin-1 has been suggested to function as a negative regulator of a variety of signaling events (Okamoto *et al*., 1998).

To investigate this hypothesis, we employed a variety of phospho-specific antibodies that have been generated against the activated forms of well-known signal transducers. It has previously been shown that these antibodies can be used to detect activated forms of a given signaling molecule by Western blotting.

Lysates from normal NIH 3T3 cells and NIH 3T3 cells harboring caveolin-1 antisense were first probed using antibodies directed against activated MEK or activated ERK. Blotting with MEK and ERK phospho-independent antibodies was performed as a control for equal loading. Figure 4A and B shows that both MEK and ERK are constitutively activated in all three caveolin-1 antisense clones. In further support of this conclusion, treatment with the well-characterized MEK inhibitor PD 98059 reduced levels of activated ERK to normal (Figure 4C). Similarly, treatment of caveolin-1 antisense clones with PD 98059 also blocked their ability to undergo anchorage-independent growth in soft agar, indicating that constitutive activation of the p42/44 MAP kinase pathway was necessary to maintain their transformed phenotype (Figure 4D). Immunoblot analysis of lysates from parental NIH 3T3 cells, Ras-transformed NIH 3T3 cells, and NIH 3T3 cells harboring caveolin-1 antisense with anti-MEK and anti-activated MEK is shown for comparison (Figure 4E). In support of these observations, we have previously shown that caveolin-1 is a natural endogenous inhibitor of both MEK and ERK (Engelman *et al*., 1998a). Thus, loss of caveolin-1 expression would be predicted to lead to constitutive activation of the p42/44 MAP kinase cascade.

How does targeted downregulation of caveolin-1 affect the cellular distribution of ERK? To answer this question, parental NIH 3T3 cells and NIH 3T3 cells harboring caveolin-1 antisense were lysed and separated into cellular (C) and nuclear (N) fractions using a standard protocol (see Materials and methods). Figure 4F (upper panel) shows that in all three caveolin-1 antisense clones the amount of total ERK is quantitatively shifted to the nucleus, while in parental NIH 3T3 cells it is predominantly excluded from the nucleus. Immunoblotting with antibodies directed against activated ERK confirmed that the nuclear fraction of ERK was indeed activated (Figure 4F, middle and lower panels). These results are as predicted based on previous studies showing that activated ERK translocates from the cytoplasm to the nucleus to phosphorylate its target substrates, such as the nuclear transcription factor Elk.

Importantly, NIH 3T3 cells harboring vector alone did not show the ability to form foci or to undergo anchorage-independent growth in soft agar (Figure 5A). Up to 10 additional vector alone controls were analyzed, and none showed a transformed phenotype (not shown). In addition, these vector alone controls did not show elevated levels of either activated MEK or activated ERK (Figure 5B). These cells also did not show any changes in the expression of caveolin-1 (not shown).

What about the SAPK/JNK or p38 MAPK pathways? Figure 6A and B shows that neither SEK or p38 MAPK are constitutively activated by targeted downregulation of caveolin-1. These results suggest that downregulation of caveolin-1 results in selective activation of the p42/44 MAPK cascade, but not the SAPK/JNK or p38 MAPK cascades. Are other cellular pathways affected by targeted downregulation of caveolin-1 protein expression? Figure 6C shows that downregulation of caveolin-1 protein expression also does not affect the amount of normal or activated CREB. Thus, downregulation of caveolin-1 only selectively affects a subset of signaling pathways.

Cell transformation induced by caveolin-1 downregulation is reversible

Interestingly, we noticed that when NIH 3T3 cell clones harboring caveolin-1 antisense were repeatedly passaged

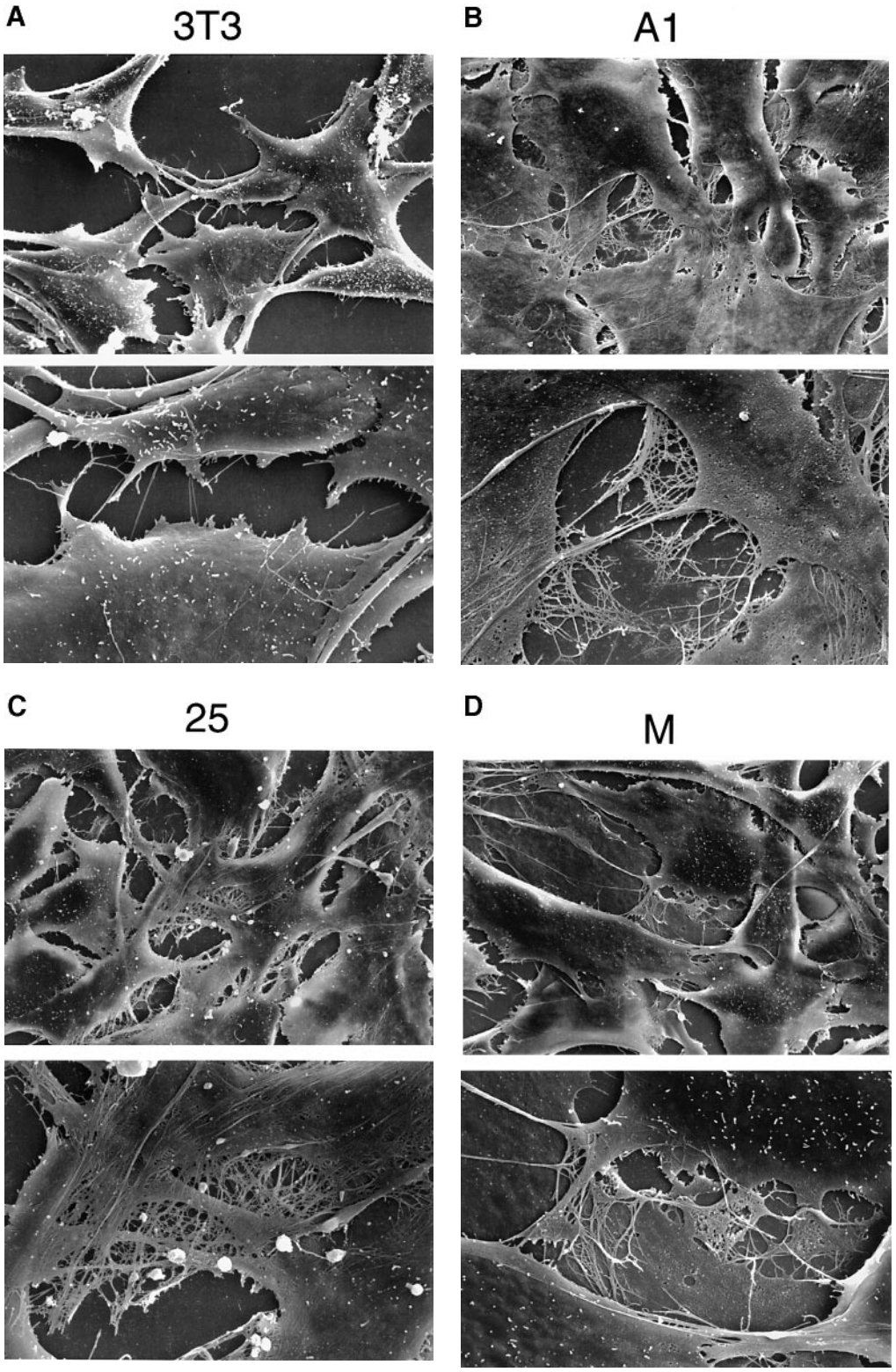

Fig. 2. NIH 3T3 cells harboring caveolin-1 antisense have increased cellular projections and appear to lose contact inhibition as seen by scanning electron microscopy. Samples were prepared for microscopy and examined using a JEOL scanning electron microscope. Each panel contains two images. The upper panel shows a view at a magnification of ×1000; the lower panel shows a higher magnification view of the same area (×3000). (**A**) NIH 3T3, (**B**) A1, (**C**) 25 and (**D**) M. Note that NIH 3T3 cells lines harboring antisense caveolin-1 (A1, 25 and M) appear crowded, suggesting a loss of contact inhibition. In addition, they appear to possess many more fine projections that are characteristic of the transformed phenotype.

in normal media lacking hygromycin or G418 (for ~4–6 passages), they reverted to the wild-type non-transformed NIH 3T3 phenotype. This indicated that selection pressure appears to be necessary to maintain the expression of the caveolin-1 antisense vector, caveolin-1 downregulation and cell transformation.

We decided to test this hypothesis directly by examining the expression of caveolin-1 sense and antisense mRNA

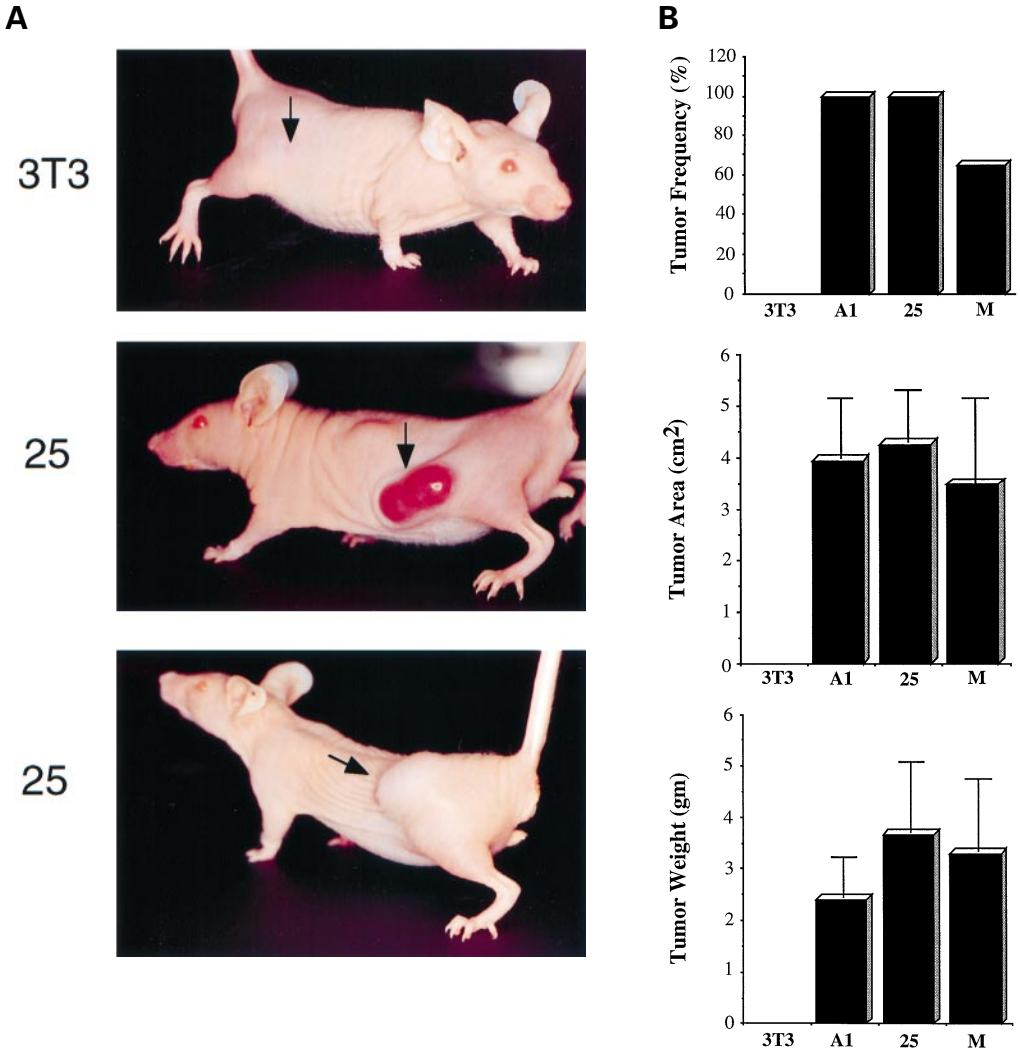

Fig. 3. NIH 3T3 cells harboring caveolin-1 antisense form tumors in nude mice. (**A**) Immunodeficient mice were injected subcutaneously with ~10^7 cells each in PBS. Mice injected with parental NIH 3T3 cells did not show the development of tumors. However, mice injected with NIH 3T3 cells lines harboring antisense caveolin-1 (A1, 25 and M) developed noticeable tumors between 1 and 2 weeks after injection. An arrow points to the injection site. Two examples are shown for mice injected with clone 25 at 14 days post-injection. (**B**) Graphical representation of tumor formation in nude mice showing frequency of tumor formation (upper), tumor area (middle) and tumor weight (lower). Quantitation was performed at 2.5–3 weeks post-injection.

species in antisense clones (A1, 25 and M) maintained with or without selection pressure. Cells maintained with selection pressure contained both sense and antisense caveolin-1 mRNAs as visualized by Northern blot analysis, and lacked caveolin-1 protein expression as seen by Western blot analysis (Figure 7A). As caveolin-1 sense mRNA was not downregulated in these cells, this indicates that caveolin-1 antisense mRNA mostly likely inhibits caveolin-1 protein expression by acting at the level of caveolin-1 translation. This is unlike the situation observed in NIH 3T3 cells transformed by activated oncogenes where caveolin-1 mRNA and protein are both specifically downregulated (Koleske *et al*., 1995).

In contrast, cells harboring caveolin-1 antisense maintained without selection pressure lost expression of caveolin-1 antisense mRNA, restoring normal levels of caveolin-1 protein expression (Figure 7A). This indicates that loss of caveolin-1 expression is reversible using this system. We next examined the phenotype of cells harboring caveolin-1 antisense and their corresponding revertants. Importantly, caveolin-1 antisense revertants lost their ability to grow in soft agar (Figure 7B) and no longer demonstrate constitutive activation of MEK and ERK (Figure 7C), as compared with the corresponding clones maintained under selection pressure. These results indicate that cell transformation induced by targeted downregulation of caveolin-1 expression is completely reversible when caveolin-1 protein levels are restored to normal.

Caveolin-1 protein expression is normally upregulated at confluency and is downregulated in rapidly dividing NIH 3T3 cells

We have shown here that targeted downregulation of caveolin-1 leads to a loss of contact inhibition. As contact inhibition normally occurs as cells become confluent, we wondered whether caveolin-1 protein expression is normally dependent on cell density. To test this idea directly, a confluent 10 cm plate of normal parental NIH 3T3 cells was trypsinized and re-plated at dilutions of 1:2,

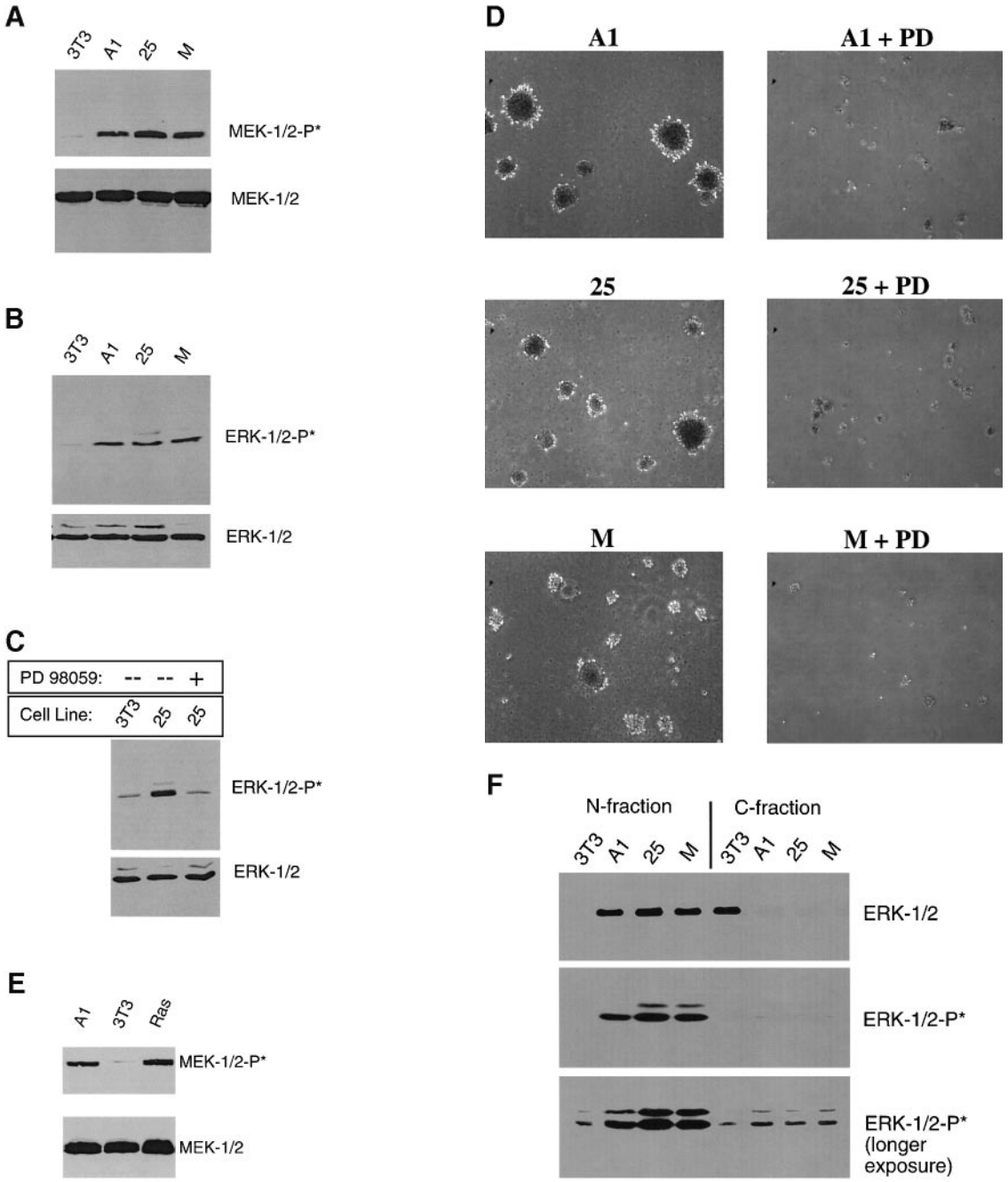

Fig. 4. MEK and ERK are constitutively activated in NIH 3T3 cells harboring caveolin-1 antisense. Lysates were prepared from parental NIH 3T3 cells and NIH 3T3 cells lines harboring antisense caveolin-1 (termed A1, 25 and M). After SDS–PAGE and transfer to nitrocellulose, immunoblotting was performed with control and phosphospecific antibody probes. (**A**) Immunoblot analysis with anti-MEK and anti-activated MEK. (**B** and **C**) Immunoblot analysis with anti-ERK and anti-activated ERK. In (C), clone 25 was treated with and without a well-characterized inhibitor of MEK (PD 98059, 50 μM) for 24 h. Treatment with this specific inhibitor of MEK reduced the level of activated ERK to normal levels. Immunoblotting with anti-MEK and anti-ERK IgG served as an additional control for equal loading. Each lane contains equal amounts of total protein. (**D**) Treatment with the MEK inhibitor (PD98059, 50 μM; indicated as PD) blocked the ability to NIH 3T3 cells harboring caveolin-1 antisense to undergo anchorage-independent growth in soft agar. (**E**) Immunoblot analysis of lysates from parental NIH 3T3 cells, Ras-transformed NIH 3T3 cells, and NIH 3T3 cells harboring caveolin-1 antisense (clone A1) with anti-MEK and anti-activated MEK is shown for comparison. (**F**) Parental NIH 3T3 cells and NIH 3T3 cells harboring caveolin-1 antisense were lysed and separated into cellular (C) and nuclear (N) fractions. Immunoblot analysis was then performed using anti-ERK (upper) and anti-activated ERK IgG (middle and lower). Two exposures of the immunoblot with activated ERK are shown. Note that in all three caveolin-1 antisense clones the amount of total ERK is quantitatively shifted to the nucleus, while in parental NIH 3T3 cells it is predominantly excluded from the nucleus. Immunoblotting with antibodies directed against activated ERK confirmed that the nuclear fraction of ERK was indeed activated. In all panels, each lane contains equal amounts of total protein.

1:7 or 1:15. After 3 days, all three sets of cells were harvested and subjected to immunoblot analysis.

Figure 8A shows that the total amount of ERK and caveolin-2 expression remains relatively constant and appears to be independent of cell density. In striking contrast, caveolin-1 protein expression is highest in con-

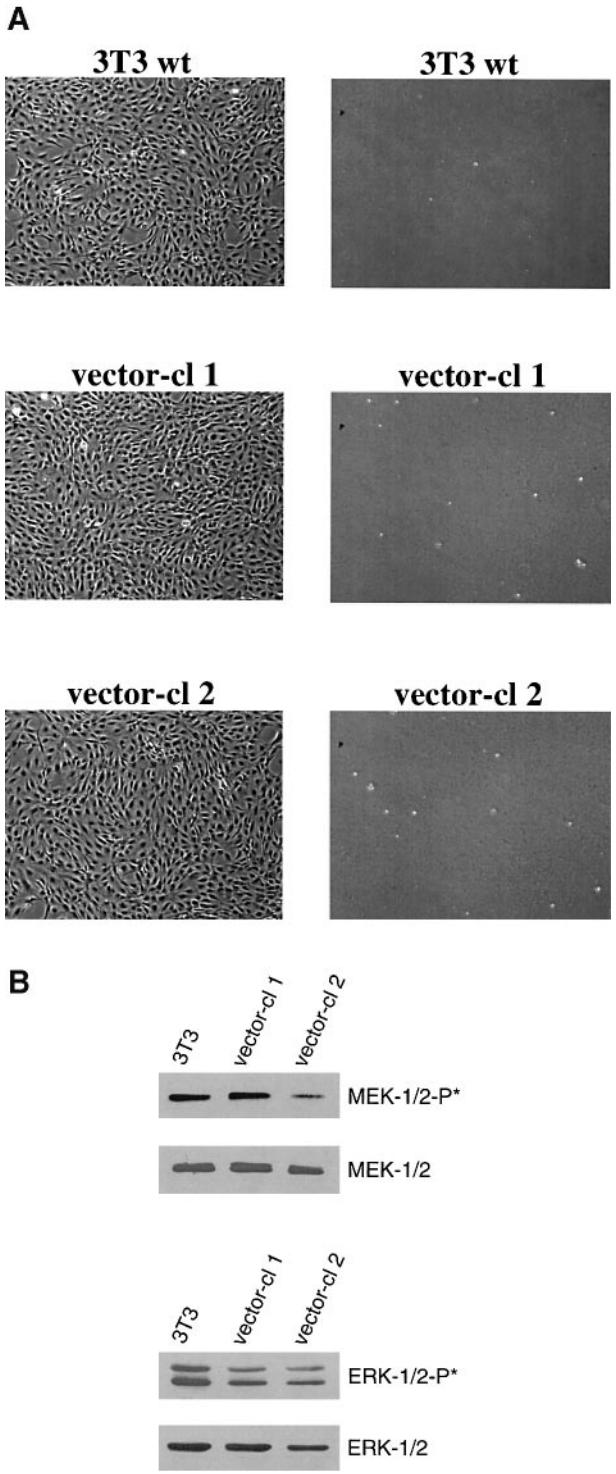

Fig. 5. Analysis of the phenotype of NIH 3T3 cells harboring vector alone. (**A**) Morphological characterization. Left panels, foci formation; right panels, growth in soft agar. Note that NIH 3T3 cells harboring vector alone behaved as parental untransfected NIH 3T3 cells. They did not exhibit foci formation or show any anchorage-independent growth in soft agar. The results obtained with two representative clones are shown here. Up to 10 additional vector alone controls were analyzed and none showed a transformed phenotype. (**B**) Western blot analysis. Activation state of MEK and ERK using phosphospecific antibody probes. Each lane contains equal amounts of total protein. Note that NIH 3T3 cells harboring vector alone did not show any elevation in the levels of activated MEK or ERK, and behaved as parental untransfected NIH 3T3 cells.

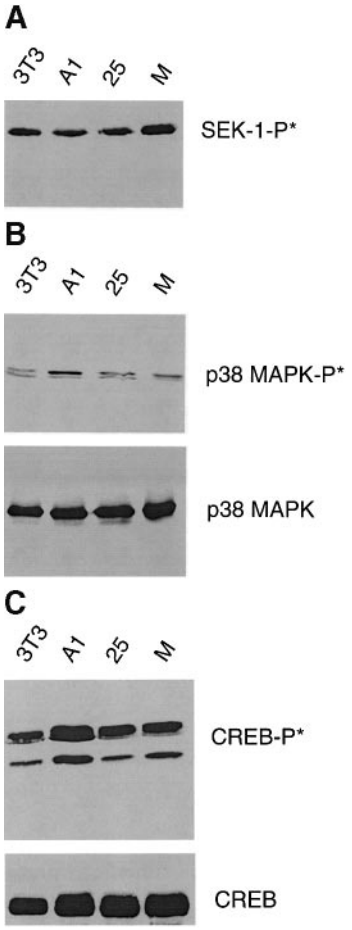

Fig. 6. Analysis of the activation state of other established signaling pathways in NIH 3T3 cells harboring caveolin-1 antisense. (A and B) Components of the SAPK/ JNK and p38 MAP kinase pathways are not activated in NIH 3T3 cells harboring caveolin-1 antisense. Lysates were prepared from parental NIH 3T3 cells and NIH 3T3 cells lines harboring antisense caveolin-1 (termed A1, 25 and M). Immunoblotting was performed with control and phosphospecific antibody probes. (**A**) Anti-activated SEK and (**B**) anti-p38 MAPK and anti-activated p38 MAPK. Each lane contains equal amounts of total protein. (**C**) CREB is not activated in NIH 3T3 cells harboring caveolin-1 antisense. Lysates were prepared from parental NIH 3T3 cells and NIH 3T3 cells lines harboring antisense caveolin-1 (termed A1, 25 and M). Immunoblotting was performed with anti-CREB and anti-activated CREB IgG. Each lane contains equal amounts of total protein.

fluent cells and is dramatically downregulated in rapidly dividing cells; conversely, activated ERK is detected primarily in rapidly dividing cells and decreases upon reaching confluency. As an additional control, we also studied the expression of a cell cycle-specific marker protein. Cyclin D1 is a marker for the G_1/S phase transition and was highest in the rapidly dividing cell population; conversely, cyclin D1 was virtually absent in the confluent cell population that expressed the highest levels of caveolin-1. Thus, activated ERK and cyclin D1 show the same pattern of expression, while caveolin-1 expression is exactly the opposite of these two markers of mitogenesis.

These results indicate that caveolin-1 protein expression is normally upregulated at high cell density, coincident with contact inhibition. This finding is consistent with the previous observation that caveolin-1 protein expression is highest in terminally differentiated cell types, such as

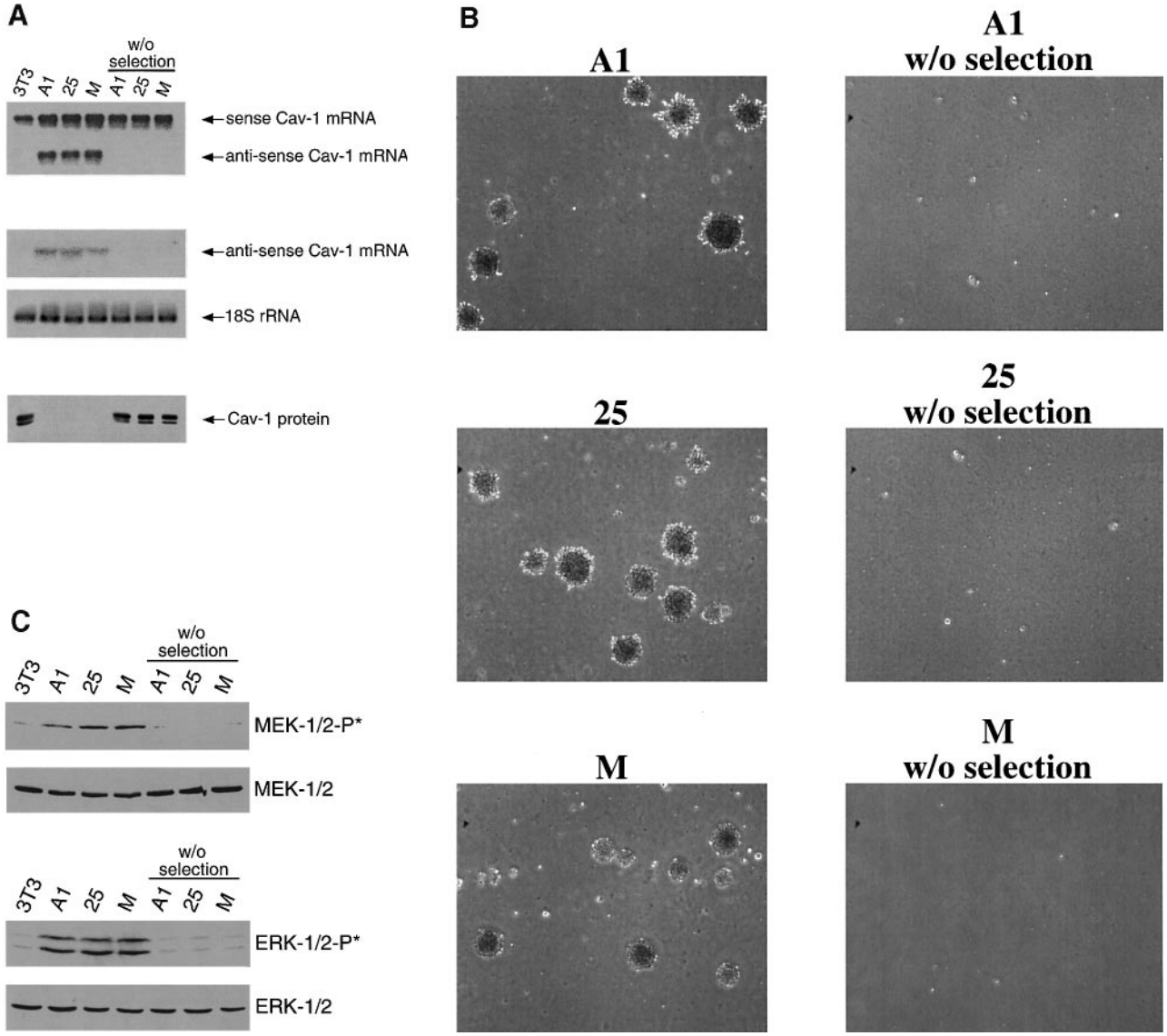

Fig. 7. Cell transformation induced by caveolin-1 downregulation is reversible. When NIH 3T3 cell clones harboring caveolin-1 antisense were repeatedly passaged in normal media lacking hygromycin or G418 (for ~4–6 passages), they appeared to revert to the wild-type non-transformed NIH 3T3 phenotype. Thus, we examined the expression of caveolin-1 sense and antisense mRNA species and caveolin-1 protein expression in antisense clones (A1, 25 and M) maintained with or without selection pressure by Northern and Western blot analysis. Also, we examined their phenotype using assays for growth in soft agar and the activation of the p42/44 MAP kinase pathway. (**A**) Northern and Western blot analysis. Northern analysis was performed with total RNA (10 μg per lane) purified from a given cell line. (Upper panel) Northern blot analysis using the cDNA to caveolin-1 as a probe. The detection of both caveolin-1 sense and antisense mRNAs is as indicated. (Middle panels) Northern blot analysis using a caveolin-1 sense oligonucleotide as the probe to detect the caveolin-1 antisense mRNA. An oligonulceotide probe to 18S rRNA was used as control for equal loading. (Lower panel) Western blot analysis using a monoclonal antibody probe to caveolin-1; each lane contains equal amounts of total protein. Note that cells maintained with selection pressure contained both sense and antisense caveolin-1 mRNAs as visualized by Northern blot analysis (upper and middle panels) and lacked caveolin-1 protein expression as seen by Western blot analysis (lower panel). In contrast, cells harboring caveolin-1 antisense maintained without selection pressure lost expression of caveolin-1 antisense mRNA (upper and middle panels), restoring normal levels of caveolin-1 protein expression (lower panel). (**B**) Growth in soft agar. Caveolin-1 antisense revertants lost their ability to grow in soft agar, as compared with the corresponding clones maintained under selection pressure. (**C**) MEK and ERK analysis. Caveolin-1 antisense revertants no longer demonstrate constitutive activation of MEK and ERK, as compared with the corresponding clones maintained under selection pressure. These results indicate that cell transformation induced by targeted downregulation of caveolin-1 expression is completely reversed when caveolin-1 protein levels are restored to normal.

adipocytes and endothelial cells (Song *et al*., 1996b; Tang *et al*., 1996; Scherer *et al*., 1997).

Figure 8B shows the localization of caveolin-1 in normal NIH 3T3 cells at different cell densities. Note that under conditions of low cell density (sparse) in which cells make no cell–cell contacts, caveolin-1 is localized mainly in a punctate or patchy distribution over the entire cell surface and within the cell interior. In contrast, when cells begin to make cell–cell contacts (sub-confluent), caveolin-1 redistributes and localizes precisely at the areas of cell–cell contact. In confluent cells, caveolin-1 localizes mainly at areas of cell–cell contact. Under these different cell density conditions, caveolin-2 also redistributes and coincides with the distribution of caveolin-1, as seen in dual-labeling studies (Figure 8C). These changes in the subcellular distribution of caveolins are consistent with a possible

role in mediating contact inhibition, as we have previously postulated (Koleske *et al*., 1995).

Serum starvation and growth factor stimulation reciprocally regulate caveolin-1 protein expression in normal NIH 3T3 cells

Given that caveolin-1 levels are downregulated by oncogenic stimuli in transformed cells (Koleske *et al*., 1995; Engelman *et al*., 1997), are downregulated in rapidly dividing cells at low density (this report), and are upregulated at confluency (this report), we next evaluated the effects of serum starvation and growth factor stimulation on the regulation of caveolin-1 expression. Based on the above studies, we would predict that caveolin-1 levels would be increased by serum starvation and dramatically decreased by the addition of growth factors to the medium.

Figure 9A shows that serum starvation of normal parental NIH 3T3 cells progressively increases caveolin-1 levels with time, while caveolin-2 levels remain relatively constant. Interestingly, upregulation of caveolin-1 expression was only observed when cells were plated at a sparse or subconfluent density prior to serum starvation; serum starvation of confluent cells had no effect on caveolin-1 expression levels (not shown).

In contrast, when serum-starved normal NIH 3T3 cells were incubated with specific growth factors (EGF, PDGF or FGF, alone or in combination) caveolin-1 levels were dramatically downregulated, while caveolin-2 levels remained relatively constant (Figure 9B). Note that the effects of PDGF and FGF (alone or in combination) were most dramatic, while little effect was observed with EGF alone. This may simply reflect different levels of a given receptor that is expressed in parental NIH 3T3 cells. However, growth factor stimulation of confluent NIH 3T3 cells had no effect on caveolin-1 expression levels (Figure 9C). Thus, caveolin-1 levels appear to be tightly regulated by the presence or absence of specific growth factor stimuli and cell density.

As growth factors such as FGF are thought to signal via receptors that are coupled to the Ras-p42/44 MAP kinase cascade, we next examined if growth factor-induced downregulation of caveolin-1 could be prevented by incubation with the MEK inhibitor PD 98059. Figure 9D shows that treatment with PD 98059 partially blocked the ability of FGF to downregulate caveolin-1. This is consistent with the idea that FGF-induced downregulation of caveolin-1 is at least in part due to activation of the p42/44 MAP kinase cascade.

Thus, downregulation of caveolin-1 in response to activation of the Ras-p42/44 MAP kinase cascade occurs both normally in response to growth factors (this report) and pathologically during cell transformation via activated oncogenes as in the case of activated Ras (G12V) (Koleske *et al*., 1995; Engelman *et al*., 1997).

Discussion

Modification and/or inactivation of caveolin-1 expression appears to be a common feature of the transformed phenotype. Historically, caveolin was first identified as a major v-Src substrate in Rous sarcoma virus transformed cells (Glenney, 1989). Based on this observation, Glenney and co-workers have proposed that caveolin may represent a critical target during cell transformation (Glenney, 1989). In direct support of this notion, caveolin-1 mRNA and protein expression are reduced or absent in NIH 3T3 cells transformed by a variety of activated oncogenes [v-Abl, Bcr-Abl, H-Ras (G12V)]; caveolae organelles are also missing from these transformed cells (Koleske *et al*., 1995). In addition, caveolin-1 expression levels correlated inversely with the ability of these cells to grow in soft agar, i.e. the cells expressing the least amount of caveolin-1 and containing no detectable caveolae formed the largest colonies in soft agar. These results identify caveolin-1 as a candidate tumor suppressor gene (Koleske *et al*., 1995). In striking contrast, the caveolin-2 protein is not downregulated in response to oncogenic transformation (Scherer *et al*., 1997).

Recently, we expressed caveolin-1 in these oncogenically transformed NIH 3T3 cells under the control of an inducible-expression system (Engelman *et al*., 1997). Regulated induction of caveolin-1 expression was monitored by Western blot analysis and immunofluorescence microscopy. Induction of caveolin-1 expression in v-Abl- and H-Ras (G12V)-transformed NIH 3T3 cells abrogated the anchorage-independent growth of these cells in soft agar, and resulted in the *de novo* formation of caveolae as seen by transmission electron microscopy (Engelman *et al*., 1997). Consistent with its antagonism of Ras-mediated cell transformation, caveolin-1 expression dramatically inhibited both Ras/MAPK-mediated and basal transcriptional activation of a mitogen-sensitive promoter (Engelman *et al*., 1997). Taken together, these results indicate that downregulation of caveolin-1 expression and caveolae organelles may be critical in maintaining the transformed phenotype in certain cell populations (Engelman *et al*., 1997).

These findings may also have relevance to human cancers. Using differential display and subtractive hybridization techniques, Sager and co-workers have identified a number of ‘candidate tumor suppressor genes’ whose mRNAs are downregulated in human mammary carcinomas (Sager *et al*., 1994). In this screening approach, caveolin-1 was independently identified as one of 26 gene products downregulated during mammary tumorigenesis. In addition, caveolin-1 expression was absent in several transformed cell lines derived from human mammary carcinomas including MT-1, MCF-7, ZR-75-1, T47D, MDA-MB-361 and MDA-MB-474 (Sager *et al*., 1994). In contrast, caveolin-1 mRNA was abundantly expressed in normal mammary epithelium. However, it remains unknown whether loss or reductions in caveolin-1 protein expression are sufficient to mediate cell transformation and/or tumorigenicity.

Here, we have employed an antisense approach to derive stable NIH 3T3 cell lines that contain normal amounts of caveolin-2, but express dramatically reduced levels of caveolin-1. NIH 3T3 cells harboring antisense caveolin-1 spontaneously formed foci, exhibited anchorage-independent growth in soft agar, formed tumors in immunodeficient mice and appeared morphologically transformed as seen by scanning electron microscopy. Biochemically, these cells also showed increased levels of activated MEK and ERK. However, the SAPK/JNK pathway, the p38 MAPK pathway and CREB were not activated in these cells. Taken together, these results

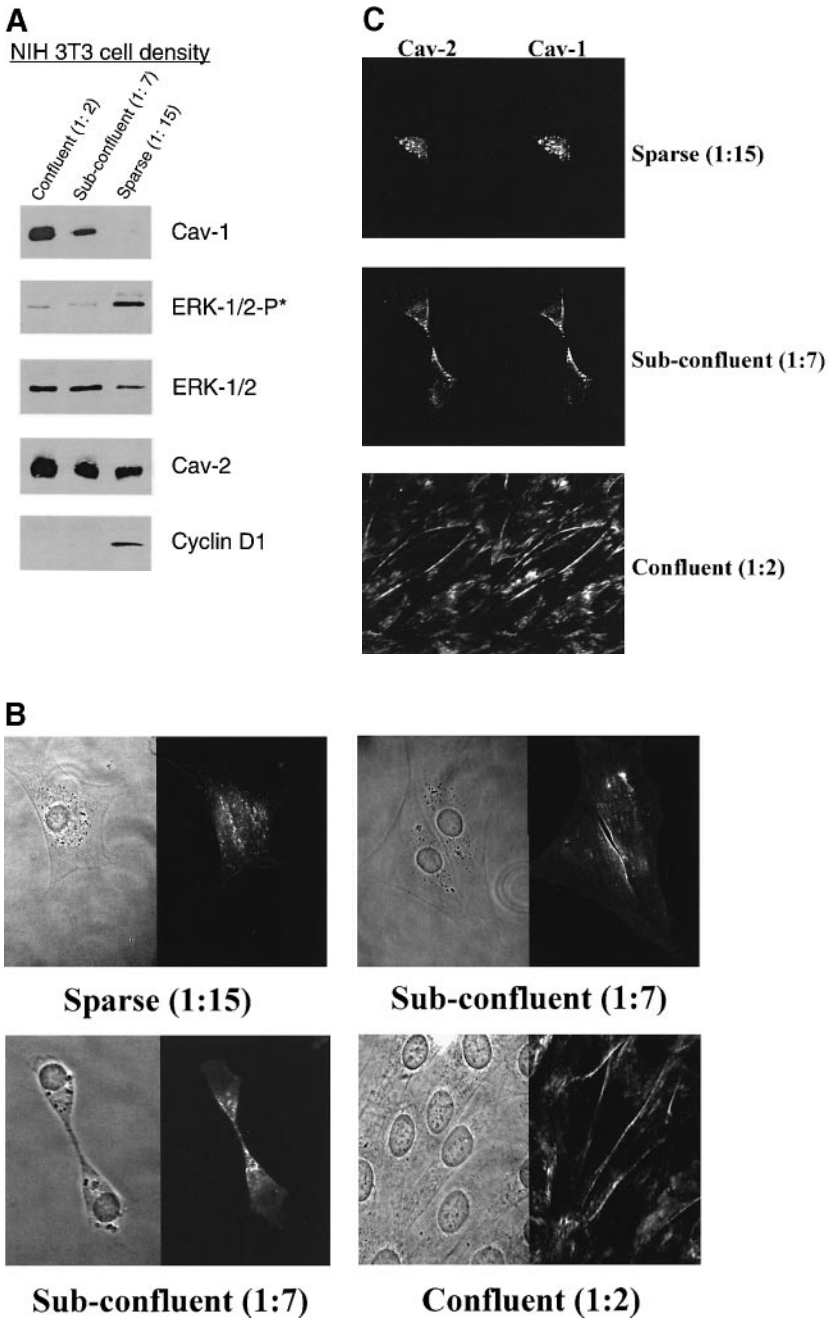

Fig. 8. Caveolin-1 protein expression is normally upregulated at confluency and is dramatically downregulated in rapid dividing NIH 3T3 cells. (**A**) Western blot analysis. A confluent 10 cm plate of parental NIH 3T3 cells was trypsinized and re-plated at dilutions of 1:2 (confluent), 1:7 (sub-confluent) or 1:15 (sparse). After 3 days, all three sets of cells were harvested and subjected to immunoblot analysis. Each lane contains equal amounts of total protein. Note that the total amount of ERK and caveolin-2 remain relatively constant. In contrast, caveolin-1 protein expression is highest in confluent cells and is dramatically downregulated in rapidly dividing cells; conversely, activated ERK is detected primarily in rapidly dividing cells and decreases upon reaching confluency. Cyclin D1, a marker for the G_1/S transition, was highest in the rapidly dividing cell population and virtually absent in confluent cells. (B) and (C) Morphological characterization. Immunolocalization of caveolins 1 and 2 in normal NIH 3T3 cells at different cell densities. Note that as the cells reach confluency, the distribution of caveolin-1 changes from a uniform punctate distribution over the entire cell surface and becomes localized primarily to areas of cell–cell contact. (**B**) Immunolabeling with anti-caveolin-1 IgG alone. (**C**) Dual-labeling with mono-specific antibodies directed against either caveolin-1 or caveolin-2. Note that the distribution of caveolin-2 follows the distribution caveolin-1.

suggest that downregulation of caveolin-1 expression is sufficient to drive oncogenic transformation and constitutively activate the p42/44 MAP kinase cascade. Importantly, cell transformation induced by targeted downregulation of caveolin-1 expression was completely reversed when caveolin-1 protein levels were restored to normal by loss of the caveolin-1 antisense vector.

These observations may be related to the ability of caveolin-1 to positively regulate contact inhibition and growth arrest in normal cells. We show here that caveolin-1 expression levels are downregulated in rapidly dividing cells and are dramatically upregulated at confluency in normal NIH 3T3 cells. These results suggest that upregulation of caveolin-1 expression levels may be important to

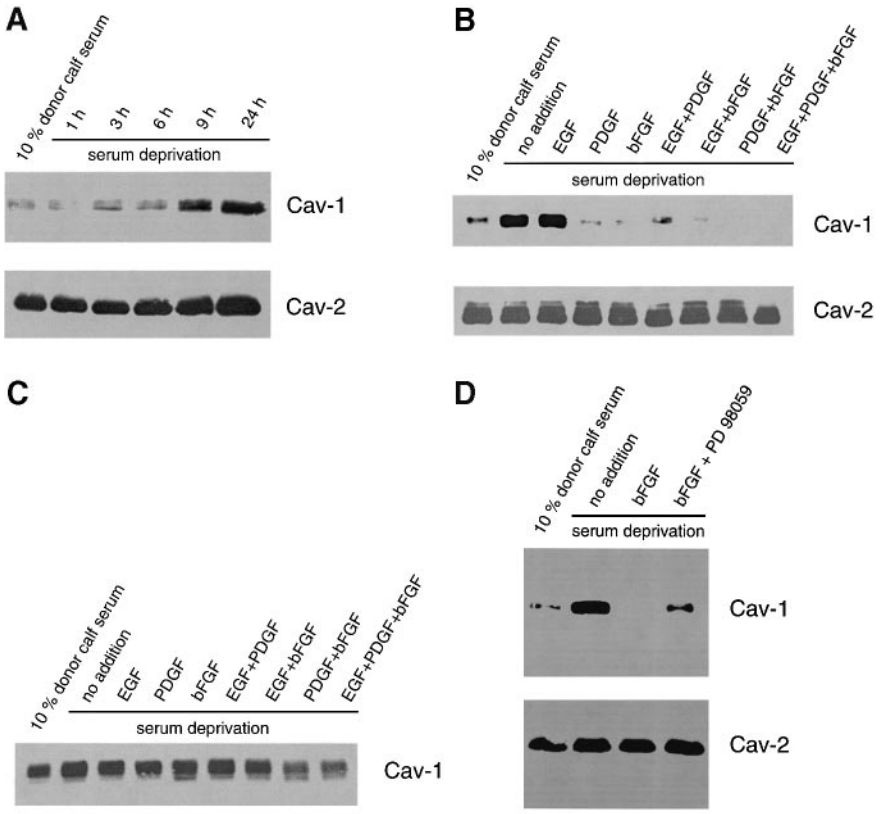

Fig. 9. Serum deprivation and growth factor stimulation reciprocally regulate caveolin-1 protein expression. (**A**) Serum deprivation of sub-confluent cells. Note that serum starvation of normal parental NIH 3T3 cells progressively increases caveolin-1 protein levels with time, while caveolin-2 levels remain relatively constant. Times are as indicated in hours. Each lane contains equal amounts of total protein. Cells grown in complete medium containing 10% donor calf serum (DCS) are also shown as a control (lane 1). (**B**) Growth factor stimulation of sub-confluent cells. Normal parental NIH 3T3 cells were incubated for 24 h with or without specific growth factors (EGF, PDGF, or FGF alone or in combination) in serum-free medium. Note that caveolin-1 protein levels were dramatically downregulated, while caveolin-2 levels remained relatively constant. The effects of PDGF and FGF (alone or in combination) were most dramatic, while little effect was observed with EGF alone. Each lane contains equal amounts of total protein. (**C**) Growth factor stimulation of confluent cells. Same as in (B), except normal parental NIH 3T3 cells were allowed to reach confluency before growth factor treatment. (**D**) Effect of the MEK inhibitor PD 98059. As in (B), normal parental NIH 3T3 cells were incubated for 24 h with or without growth factor (FGF alone or in combination with PD 98059) in serum-free medium. Note that treatment with PD 98059 partially blocked the ability of FGF to downregulate caveolin-1. In all panels, each lane contains equal amounts of total protein.

mediate normal contact inhibition and to negatively regulate the activation state of the p42/44 MAP kinase cascade. In support of these findings, it has been shown that caveolins are most abundantly expressed in terminally differentiated cell types such as endothelial cells, adipocytes and muscle cells, and are dramatically upregulated during adipogenesis and myotube formation (Way and Parton, 1995; Song *et al*., 1996b; Tang *et al*., 1996; Scherer *et al*., 1997).

In accordance with our current observations, several independent laboratories have now shown that components of the p42/44 MAP kinase cascade, including MEK and ERK, are concentrated within caveolae membranes by employing both *in vitro* biochemical methods and *in vivo* immunolabeling techniques (Liu *et al*., 1996, 1997a,b; Mineo *et al*., 1996; Song *et al*., 1996a). For example, morphological studies have directly shown that ERK-1/2 is concentrated in plasma membrane caveolae *in vivo* using immunoelectron microscopy (Liu *et al*., 1997b). However, the functional significance of the caveolar localization of the p42/44 MAP kinase cascade has remained unknown.

How might the downregulation of caveolin-1 protein expression activate the p42/44 MAP kinase cascade? Recently, Anderson and colleagues have shown that the pool of ERK-1 that localizes to caveolae is initially inactive and can be activated by regulated stimulation with growth factor ligands, such as PDGF (Liu *et al*., 1997b). After such stimulation, ERK-1 is activated and translocates from the caveolae membrane to the cytosol, suggesting that ERK-1 is activated as it leaves the caveolae membrane (Liu *et al*., 1997b). These results are consistent with our current findings that downregulation of caveolin-1 expression constitutively activates signaling from MEK and ERK *in vivo*, perhaps by prematurely releasing activated ERK-1/2 and other components of the p42/44 MAP kinase cascade into the cytosol so that they may accumulate within the nucleus. The data presented in Figure 4F provide direct support for this hypothesis.

In further support of this hypothesis, we have shown that transient co-expression of caveolin-1 with activated H-Ras (G12V) blocks its ability to transcriptionally activate a mitogen sensitive promoter *in vivo* (Engelman *et al*., 1997). As mutational activation of H-Ras prevents or destabilizes its interaction with caveolin-1 (Song *et al*., 1996a), caveolin-1 must exert its effects on one or more of the downstream targets of H-Ras, such as Raf-1, MEK-1/2 or ERK-1/2. In accordance with this idea, we have

recently shown that (i) transient co-expression with caveolin-1 dramatically inhibits signaling from Raf-1, MEK-1 and ERK-2 to the nuclear transcription factor Elk *in vivo*, and (ii) peptides derived caveolin-1 inhibit the *in vitro* kinase activity of purified MEK-1 and ERK-2 (Engelman *et al*., 1998a). Thus, over-expression of caveolin-1 can inhibit signal transduction from the p42/44 MAP kinase cascade via a direct interaction of caveolin-1 with MEK and ERK (Engelman *et al*., 1998a), while targeted downregulation of caveolin-1 is sufficient to constitutively activate the p42/44 MAP kinase cascade (this report).

Based on our current and previous observations, we suggest that a novel form of negative reciprocal regulation exists between p42/44 MAP kinase activation and caveolin-1 protein expression. The evidence is as follows: (i) upregulation of caveolin-1 protein expression downregulates p42/44 MAP kinase activity (Engelman *et al*., 1998a), i.e. transient co-expression of caveolin-1 with MEK or ERK inhibits their ability to transcriptionally activate an *in vivo* Elk-luciferase reporter system in CHO cells; (ii) downregulation of caveolin-1 protein expression upregulates p42/44 MAP kinase activity (this report), i.e. expression of caveolin-1 antisense downregulates caveolin-1 protein expression in NIH 3T3 cells and leads to constitutive activation of MEK and ERK; (iii) upregulation p42/44 MAP kinase activity downregulates caveolin-1 mRNA and protein expression (Koleske *et al*., 1995; Engelman *et al*., 1997), i.e. expression of activated Ras (G12V) in NIH 3T3 cells leads to a loss of caveolin-1 mRNA and protein expression; and (iv) downregulation of p42/44 MAP kinase activity upregulates caveolin-1 protein expression (Engelman *et al*., 1997), i.e. treatment of Ras-transformed NIH 3T3 cells with the MEK inhibitor (PD98059) restores the expression of caveolin-1 protein to normal levels observed in non-transformed NIH 3T3 cells. Importantly, these four independent observations are consistent with the changes we observed in caveolin-1 protein levels in response to cell density, growth factor deprivation, and growth factor stimulation in normal NIH 3T3 cells (Figures 8 and 9).

Recently, the gene encoding caveolin-1 has been found to map to the q31 region of human chromosome 7 and the A-2 region of mouse chromosome 6 (Engelman *et al*., 1998c,d). Interestingly, human chromosome 7q31 and murine chromosome 6-A2 are often deleted or are translocational break point sites in a wide variety of tumors. Such tumors include hepatomas (Zenklusen *et al*., 1996, 1997), ovarian cancers (Kerr *et al*., 1996; Koike *et al*., 1997), prostate cancers (Huang *et al*., 1998; Jenkins *et al*., 1998), uterine leiomyomas (Ishwad *et al*., 1997), myeloid neoplasms (Liang *et al*., 1998), oral cancers (Wang *et al*., 1998), breast cancers (Huang *et al*., 1998), stomach adenocarcinomas (Nishizuka *et al*., 1997) and renal cell carcinomas (Shridhar *et al*., 1997). Based on these studies, it has been concluded that an as yet unidentified tumor suppressor gene resides at 7q31/6-A2.

The unidentified tumor suppressor gene located at 7q31/6A-2 may be caveolin-1 given that: (i) the caveolin-1 gene is localized to this chromosomal region; (ii) caveolin-1 mRNA and protein are downregulated in during cell transformation of cultured NIH 3T3 cells, in transgenic mouse models of breast cancer and in cell lines derived from human breast cancers (Sager *et al*., 1994; Koleske *et al*., 1995; Engelman *et al*., 1997, 1998b; Lee *et al*., 1998); (iii) recombinant expression of caveolin-1 in transformed NIH 3T3 cells or cell lines derived from human breast cancers can suppress their transformed phenotype, such as anchorage-independent growth in soft agar (Engelman *et al*., 1997; Lee *et al*., 1998); and (iv) loss of caveolin-1 expression is sufficient to mediate cell transformation and tumorigenicity (this report). As many normal adult tissues express caveolin-1, it will be important to determine whether any of these chromosomal rearrangements lead to a loss of caveolin-1 mRNA or protein expression during tumorigenesis.

Materials and methods

Materials

Antibodies and their sources were as follows: anti-caveolin-1 IgG [mAb 2297; gift of Dr John R.Glenney Jr, Transduction Laboratories; (Scherer *et al*., 1995)]; anti-caveolin-2 IgG [mAb 65; gift of Dr John R.Glenney Jr, Transduction Laboratories; (Scherer *et al*., 1997)]; anti-ERK-1/2; anti-activated ERK-1/2; anti-MEK-1/2; anti-activated MEK-1/2; anti-activated SEK-1; anti-p38 MAPK; anti-activated p38 MAPK; anti-CREB; anti-phospho-CREB (New England Biolabs, Inc.). The MEK-1/2 inhibitor (PD 98059) was purchased from Calbiochem, Inc. The cDNA for murine caveolin-1 was as we described previously (Tang *et al*., 1994). The antibody directed against cyclin D1 (HD1) was the generous gift of Drs J.Koh and E.Harlow (Massachusetts General Cancer Center). Growth factors (EGF, PDGF-BB, and bFGF) were purchased from Upstate Biotechology, Inc.

Cell culture

NIH 3T3 cells were grown in DME supplemented with glutamine, antibiotics (penicillin and streptomycin) and 10% DCS, as previously described (Koleske *et al*., 1995; Engelman *et al*., 1997).

Construction of caveolin-1 antisense vectors

The full-length untagged cDNA encoding murine caveolin-1 was inserted in the antisense orientation into two different expression vectors that were either driven by a CMV-based promoter (pCB6, containing a neomycin resistance marker; gift of J.Casanova, MGH) or the β-actin promoter (pCAGGS, gift of Dr Armin Rehm, Ploegh Laboratory, Harvard Medical School, MA). pCAGGS constructs were co-transfected with a plasmid containing hygromycin resistance (pCB7).

Establishment of stable NIH 3T3 cells lines harboring caveolin-1 antisense

Parental NIH 3T3 cells were transfected with caveolin-1 antisense vectors using a modified calcium phosphate precipitation protocol. Resistant clones were selected using hygromycin B (200 μg/ml) or G418 (350 μg/ml). Individual clones were isolated using cloning rings. Lysates were prepared and assayed for reductions in the expression of caveolin-1 by immunoblotting. Mock transfected or NIH 3T3 cells transfected with empty vector alone served as a positive control. Revertants of NIH 3T3 cell clones harboring antisense caveolin-1 were derived by culturing these clonal cell lines in the absence of selection medium for 4–6 passages.

Assays for foci formation and growth in soft agar

Foci formation was assessed by plating the cells at high density (~10^7 cells) in 10 cm dishes. Two days after plating, cells were photographed. Ras-transformed NIH 3T3 cells were used as a positive control for foci formation. Growth in soft agar was assayed as we described previously, with minor modifications (Koleske *et al*., 1995). Briefly, 2.5×10^4 cells of each cell line were suspended in 3 ml of DMEM containing 10% DCS and 0.33% SeaPlaque low-melting temperature agarose. These cells were plated over a 2 ml layer of solidified DMEM containing 10% DCS and 0.5% agarose, and cells were allowed to settle to the interface between these layers at 37°C. After 20 min, the plates were allowed to harden at room temperature for 30 min before returning to 37°C. The plates were fed every 2–3 days by overlaying with 2 ml of medium containing 0.33% agarose. After 10–14 days, colonies were photographed under low magnification (×4 or ×6). For each cell line, the number of

colonies in seven random fields at the same magnification was counted for quantitation purposes.

Scanning electron microscopy

Cells were grown on glass coverslips and fixed in 2.5% paraformaldehyde, 0.1 M sodium cacodylate pH 7.4. After dehydration through a graded series of ethanol, cells were subjected to critical point drying using liquid carbon dioxide in a Tousimis Samdri 790 Critical Point Drier (Rockville, MD). Cells were then sputter coated with gold-palladium in a Denton Vacuum Desk-1 Sputter Coater (Cherry Hill, NJ). Samples were then examined with a JEOL JSM6400 Scanning Electron Microscope (Peabody, MA), using an accelerating voltage of 10 kV.

Tumorigenicity in immunodeficient mice

Male, 6- to 8-week old, nude mice were obtained from the National Cancer Institute (BALB/cAnNCr-nuBR) or Charles River Laboratories [Nu/Nu (CD-1) BR]. Briefly, NIH 3T3 cells, suspended in sterile phosphate-buffered saline (PBS), were injected subcutaneously into each flank of the nude mice. For each mouse, one flank was injected with control NIH 3T3 cells while the other flank received NIH 3T3 cells that harbor an antisense caveolin-1 construct. Thus, each mouse received two injections of 10^7 cells in 0.1–0.3 ml of PBS. Tumor growth localized to the site of injection was monitored. Mice were sacrificed 2–3 weeks after injection. Any tumors which formed were measured and excised, and their weight was recorded. Four to eight mice were used to evaluate the tumorigenicity of a given cell line.

Immunoblotting with phosphospecific antibody probes

Cells were lysed in boiling sample buffer, as suggested by the manufacturer of phosphospecific antibody probes (New England Biolabs, Inc.). Samples were then collected and boiled for a total of 5 min. Samples were homogenized using a 26 g needle and a 1 ml syringe. After SDS–PAGE (12.5% acrylamide) and transfer to nitrocellulose (0.2 μm), blots were probed with primary antibodies (dilution of 1:500; New England Biolabs, Inc.) and the appropriate HRP-conjugated secondary antibody (dilution of 1:5000; Transduction Laboratories). Bound antibodies were visualized using ECL (Amersham, Inc.).

Nuclear fractionation

Separation of nuclei from other cellular remnants was carried out as described previously using a standard protocol (Dignam *et al*., 1983). Briefly, NIH 3T3 cells were collected and washed once with PBS. Cells were then resuspended in 2 vol. of ice-cold buffer A (10 mM HEPES pH 7.9; 1.5 mM $MgCl_2$; 10 mM KCl; 0.5 mM DTT; 0.5 mM PMSF) and homogenized using a Dounce homogenizer (20 strokes; B-type pestle). The homogenate was viewed microscopically to ensure that cell lysis had occurred. The nuclear fraction (designated N-fraction) was separated from the remaining cell lysate (designated C-fraction) by centrifugation at 1000 *g* for 10 min at 4°C. Samples were then separated by SDS–PAGE (12.5% acrylamide).

Immunostaining of NIH 3T3 cells

Normal parental NIH 3T3 cells were washed three times with PBS and fixed for 30 min at room temperature with 2% paraformaldehyde in PBS. Fixed cells were rinsed with PBS and permeabilized with 0.1% Triton X-100, 0.2% bovine serum albumin (BSA) for 10 min. Cells were then treated with 25 mM NH_4Cl in PBS for 10 min at room temperature to quench free aldehyde groups. The cells were rinsed with PBS and incubated with primary antibodies for 1 h at room temperature: either anti-caveolin 1 IgG (pAb; directed against caveolin-1 residues 2–21; Santa Cruz Biotech, Inc.), and/ or anti-caveolin 2 IgG [mAb clone 65, Transduction Laboratories; (Scherer *et al*., 1997)] diluted into PBS with 0.1% Triton X-100, 0.2% BSA. After three washes with PBS (10 min each), cells were incubated with the secondary antibodies for 1 h at room temperature: lissamine rhodamine B sulfonyl chloride-conjugated goat anti-rabbit antibody (5 μg/ml) and fluorescein isothiocyanate-conjugated goat anti-mouse antibody (5 μg/ml). Cells were washed three times with PBS (10 min for each wash). Slides were mounted with slow-Fade anti-fade reagent and examined by confocal microscopy.

Northern blot analysis

Total RNA was extracted from one 10 cm dish of cells using the RNeasy Mini Kit (Qiagen). Ten micrograms of total RNA was then used for Northern blot analysis. The following two oligonucleotides were used as probes to detect caveolin-1 sense and antisense mRNAs, respectively: 5′-TACAGACCCCCGTTTATGCACCTGAGG-3′ and 5′-AGTATAGAGAAAGACGCACGACTACGC-3′. The full-length murine caveolin-1 cDNA was also used as a probe to detect both caveolin-1 sense and antisense mRNA species. We used the following oligonucleotide probe to detect 18S rRNA as a control for equal loading: 5′-CTTCCTCTAGATAGTCAAGTTCGACCGTCT-3′.

Serum starvation and growth factor stimulation of parental NIH 3T3 cells

A 10 cm plate of confluent normal NIH 3T3 cells was trypsinized, re-plated at dilution of 1:15 (sparse), and after one day of culture, complete medium was replaced with medium without serum. Cells were then grown in medium without serum for 1, 3, 6, 9 and 24 h, harvested, and subjected to immunoblot analysis. In the growth factor stimulation experiments, normal parental NIH 3T3 cells were grown in medium without serum for 24 h in presence or absence of EGF (10 ng/ml), PDGF-BB (10 ng/ml) and bFGF (5 ng/ml) alone or in combination.

Acknowledgements

We thank Drs Frank Macaluso and Leslie Gunther for their expert assistance with scanning electron microscopy, Drs Winfried Edelmann and Han-Woong Lee for help with photography, and Drs J.R.Glenney Jr, J.Koh and E.Harlow for generously donating antibody probes. This work was supported by an NIH FIRST Award (GM-50443), grants from the G.Harold and Leila Y.Mathers Charitable Foundation, the Charles E.Culpeper Foundation and the Sidney Kimmel Foundation for Cancer Research, all to M.P.L. R.G.P. was supported by National Institute of Health grants R29-CA70897, R01-CA75503 and an award from the Susan Komen foundation. G.W. was supported in part by a Travel Fellowship from the Aichi Health Promotion Foundation, the Owari kenyu-kai and the Takasu Foundation. J.A.E. was supported by an NIH Medical Scientist Training Program grant T32-GM07288.

References

Bretscher,M. and Whytock,S. (1977) Membrane-associated vesicles in fibroblasts. *J. Ultrastruc. Res*., **61**, 215–217.

Couet,J., Li,S., Okamoto,T., Scherer,P.S. and Lisanti,M.P. (1997a) Molecular and cellular biology of caveolae: paradoxes and plasticities. *Trends Cardiovasc. Med*., **7**, 103–110.

Couet,J., Li,S., Okamoto,T., Ikezu,T. and Lisanti,M.P. (1997b) Identification of peptide and protein ligands for the caveolin-scaffolding domain. Implications for the interaction of caveolin with caveolae-associated proteins. *J. Biol. Chem*., **272**, 6525–6533.

Couet,J., Sargiacomo,M. and Lisanti,M.P. (1997c) Interaction of a receptor tyrosine kinase, EGF-R, with caveolins. Caveolin binding negatively regulates tyrosine and serine/threonine kinase activities. *J. Biol. Chem*., **272**, 30429–30438.

Dignam,J.D., Lebovitz,R.M. and Roeder,R.G. (1983) Accurate transcription initiation by RNA polymerase II in a soluble extract from isolated mammalian nuclei. *Nucleic Acids Res*., **11**, 1475–1489.

Engelman,J.A., Wycoff,C.C., Yasuhara,S., Song,K.S., Okamoto,T. and Lisanti,M.P. (1997) Recombinant expression of caveolin-1 in oncogenically transformed cells abrogates anchorage-independent growth. *J. Biol. Chem*., **272**, 16374–16381.

Engelman,J.A., Chu,C., Lin,A., Jo,H., Ikezu,T., Okamoto,T., Kohtz,D.S. and Lisanti,M.P. (1998a) Caveolin-mediated regulation of signaling along the p42/44 MAP kinase cascade *in vivo*. A role for the caveolin-scaffolding domain. *FEBS Lett*., **428**, 205–211.

Engelman,J.A. *et al*. (1998b) Reciprocal regulation of Neu tyrosine kinase activity and caveolin-1 protein expression *in vitro* and *in vivo*. Implications for human breast cancer. *J. Biol. Chem*., **273**, 20448–20455.

Engelman,J.A., Zhang,X.L., Galbiati,F. and Lisanti,M.P. (1998c) Chromosomal localization, genomic organization and developmental expression of the murine caveolin gene family (Cav-1, -2 and -3). Cav-1 and Cav-2 genes map to a known tumor suppressor locus (6-A2/7q31). *FEBS Lett*., **429**, 330–336.

Engelman,J.A., Zhang,X.L. and Lisanti,M.P. (1998d) Genes encoding human caveolin-1 and -2 are co-localized to the D7S522 locus (7q31.1), a known fragile site (FRA7G) that is frequently deleted in human cancers. *FEBS Lett*., **436**, 403–410.

Fan,J.Y., Carpentier,J.-L., van Obberghen,E., Grunfeld,C., Gorden,P. and Orci,L. (1983) Morphological changes of the 3T3-L1 fibroblast plasma membrane upon differentiation to the adipocyte form. *J. Cell Sci.*, **61**, 219–230.

Forbes,M.S., Rennels,M. and Nelson,E. (1979) Caveolar systems and sarcoplasmic reticulum in coronary smooth muscle cells. *J. Ultrastruc. Res*., **67**, 325–339.

Fra,A.M., Masserini,M., Palestini,P., Sonnino,S. and Simons,K. (1995a) A photo-reactive derivative of ganglioside GM1 specifically cross-links VIP21-caveolin on the cell surface. *FEBS Lett.*, **375**, 11–14.

Fra,A.M., Williamson,E., Simons,K. and Parton,R.G. (1995b) *De novo* formation of caveolae in lymphocytes by expression of VIP21-caveolin. *Proc. Natl Acad. Sci. USA*, **92**, 8655–8659.

Furuchi,T. and Anderson,R.G.W. (1998) Cholesterol depletion of caveolae causes hyperactivation of extracellular signal-related kinase (ERK). *J. Biol. Chem*., **273**, 21099–21104.

Garcia-Cardena,G., Oh,P., Liu,J., Schnitzer,J.E. and Sessa,W.C. (1996) Targeting of nitric oxide synthase to endothelial cell caveolae via palmitoylation: implications for caveolae localization. *Proc. Natl Acad. Sci. USA*, **93**, 6448–6453.

Garcia-Cardena,G., Martasek,P., Siler-Masters,B.S., Skidd,P.M., Couet,J.C., Li,S., Lisanti,M.P. and Sessa,W.C. (1997) Dissecting the interaction between nitric oxide synthase (NOS) and caveolin: functional significance of the NOS caveolin binding domain *in vivo*. *J. Biol. Chem*., **272**, 25437–25440.

Glenney,J.R. (1989) Tyrosine phosphorylation of a 22 kDa protein is correlated with transformation with Rous sarcoma virus. *J. Biol. Chem*., **264**, 20163–20166.

Glenney,J.R. (1992) The sequence of human caveolin reveals identity with VIP 21, a component of transport vesicles. *FEBS Lett*., **314**, 45–48.

Glenney,J.R. and Soppet,D. (1992) Sequence and expression of caveolin, a protein component of caveolae plasma membrane domains phosphorylated on tyrosine in RSV-transformed fibroblasts. *Proc. Natl Acad. Sci. USA*, **89**, 10517–10521.

Huang,H., Qian,C., Jenkins,R.B. and Smith,D.I. (1998) FISH mapping of YAC clones at human chromosomal band 7q31.2: identification of YACS spanning FRA7G within the common region of LOH in breast and prostate cancer. *Genes Chromosom. Cancer*, **21**, 152–159.

Ishwad,C.S., Ferrell,R.E., Hanley,K., Davare,J., Meloni,A.M., Sandberg, A.A. and Surti,U. (1997) Two discrete regions of deletion at 7q in uterine leiomyomas. *Genes Chromosom. Cancer*, **19**, 156–160.

Jenkins,R., Takahashi,S., DeLacey,K., Bergstralh,E. and Lieber,M. (1998) Prognostic significance of allelic imbalance of chromosome arms 7q, 8p,16q and 18q in stage T3N0M0 prostate cancer. *Genes Chromosom. Cancer*, **21**, 131–143.

Ju,H., Zou,R., Venema,V.J. and Venema,R.C. (1997) Direct interaction of endothelial nitric-oxide synthase and caveolin-1 inhibits synthase activity. *J. Biol. Chem*., **272**, 18522–18525.

Kerr,J. *et al.* (1996) Allelic loss on chromosome 7q in ovarian adenocarcinomas: two critical regions and a rearrangement of the PLANH1 locus. *Oncogene*, **13**, 1815–1818.

Koike,M., Takeuchi,S., Yokota,J., Park,S., Hatta,Y., Miller,C.W., Tsuruoka,N. and Koeffler,H.P. (1997) Frequent loss of heterozygosity in the region of the D7S523 locus in advanced ovarian cancer. *Genes Chromosom. Cancer*, **19**, 1–5.

Koleske,A.J., Baltimore,D. and Lisanti,M.P. (1995) Reduction of caveolin and caveolae in oncogenically transformed cells. *Proc. Natl Acad. Sci. USA*, **92**, 1381–1385.

Kurzchalia,T., Dupree,P., Parton,R.G.,Kellner,R., Virta,H., Lehnert,M. and Simons,K. (1992) VIP 21, A 21-kDa membrane protein is an integral component of trans-Golgi-network-derived transport vesicles. *J. Cell Biol*., **118**, 1003–1014.

Lee,S.W., Reimer,C.L., Oh,P., Campbell,D.B. and Schnitzer,J.E. (1998) Tumor cell growth inhibition by caveolin re-expression in human breast cancer cells. *Oncogene*, **16**, 1391–1397.

Li,S., Okamoto,T., Chun,M., Sargiacomo,M., Casanova,J.E., Hansen, S.H., Nishimoto,I. and Lisanti,M.P. (1995) Evidence for a regulated interaction between hetero-trimeric G proteins and caveolin. *J. Biol. Chem*., **270**, 15693–15701.

Li,S., Couet,J. and Lisanti,M.P. (1996a) Src tyrosine kinases, G alpha subunits and H-Ras share a common membrane-anchored scaffolding protein, Caveolin. Caveolin binding negatively regulates the auto-activation of Src tyrosine kinases. *J. Biol. Chem*., **271**, 29182–29190.

Li,S., Song,K.S. and Lisanti,M.P. (1996b) Expression and characterization of recombinant caveolin: Purification by poly-histidine tagging and cholesterol-dependent incorporation into defined lipid membranes. *J. Biol. Chem*., **271**, 568–573.

Li,S., Galbiati,F., Volonte,D., Sargiacomo,M., Engelman,J.A., Das,K., Scherer,P.E. and Lisanti,M.P. (1998) Mutational analysis of caveolin-induced vesicle formation. Expression of caveolin-1 recruits caveolin-2 to caveolae membranes. *FEBS Lett*., **434**, 127–134.

Liang,H., Fairman,J., Claxton,D.F., Nowell,P.C., Green,E.D. and Nagarajan,L. (1998) Molecular anatomy of chromosome 7q deletions in myeloid neoplasms: evidence for multiple critical loci. *Proc. Natl Acad. Sci. USA*, **95**, 3781–3785.

Lisanti,M.P., Scherer,P., Tang,Z.-L. and Sargiacomo,M. (1994a) Caveolae, caveolin and caveolin-rich membrane domains: a signalling hypothesis. *Trends Cell Biol*., **4**, 231–235.

Lisanti,M.P., Scherer,P.E., Vidugiriene,J., Tang,Z.-L., Hermanoski-Vosatka,A., Tu,Y.-H., Cook,R.F. and Sargiacomo,M. (1994b) Characterization of caveolin-rich membrane domains isolated from an endothelial-rich source: implications for human disease. *J. Cell Biol*., **126**, 111–126.

Liu,P., Ying,Y., Ko,Y.-G. and Anderson,R.G.W. (1996) Localization of the PDGF-stimulated phosphorylation cascade to caveolae. *J. Biol. Chem*., **271**, 10299–10303.

Liu,J., Oh,P., Horner,T., Rogers,R.A. and Schnitzer,J.E. (1997a) Organized endothelial cell signal transduction in caveolae. *J. Biol. Chem*., **272**, 7211–7222.

Liu,P., Ying,Y.S. and Anderson,R.G.W. (1997b) PDGF activates MAP kinase in isolated caveolae. *Proc. Natl Acad. Sci. USA*, **94**, 13666–13670.

Michel,J.B., Feron,O., Sase,K., Prabhakar,P. and Michel,T. (1997) Caveolin versus Calmodulin. Counterbalancing allosteric modulators of endothelial nitric oxide synthase. *J. Biol. Chem*., **272**, 25907–25912.

Mineo,C., James,G.L., Smart,E.J. and Anderson,R.G.W. (1996) Localization of EGF-stimulated Ras/Raf-1 interaction to caveolae membrane. *J. Biol. Chem*., **271**, 11930–11935.

Murata,M., Peranen,J., Schreiner,R., Weiland,F., Kurzchalia,T. and Simons,K. (1995) VIP21/caveolin is a cholesterol-binding protein. *Proc. Natl Acad. Sci. USA*, **92**, 10339–10343.

Nishizuka,S., Tamura,G., Terashima,M. and Satodate,R. (1997) Commonly deleted region on the long arm of chromosome 7 in differentiated adenocarcinoma of the stomach. *Br. J. Cancer*, **76**, 1567–1571.

Oka,N., Yamamoto,M., Schwencke,C., Kawabe,J., Ebina,T., Couet,J., Lisanti,M.P. and Ishikawa,Y. (1997) Caveolin interaction with protein kinase C: isoenzyme-dependent regulation of kinase activity by the caveolin-scaffolding domain peptide. *J. Biol. Chem*., **272**, 33416–33421.

Okamoto,T., Schlegel,A., Scherer,P.E. and Lisanti,M.P. (1998) Caveolins, a family of scaffolding proteins for organizing 'pre-assembled signaling complexes' at the plasma membrane. *J. Biol. Chem*., **273**, 5419–5422.

Rothberg,K.G., Heuser,J.E., Donzell,W.C., Ying,Y., Glenney,J.R. and Anderson,R.G.W. (1992) Caveolin, a protein component of caveolae membrane coats. *Cell*, **68**, 673–682.

Sager,R. *et al*. (1994) RNA genetics of breast cancer: maspin as a paradigm. *Cold Spring Harbor Symp. Quant. Biol*., **LIX**, 537–546.

Sargiacomo,M., Scherer,P.E., Tang,Z.-L., Kubler,E., Song,K.S., Sanders, M.C. and Lisanti,M.P. (1995) Oligomeric structure of caveolin: Implications for caveolae membrane organization. *Proc. Natl. Acad. Sci. USA*, **92**, 9407–9411.

Scherer,P.E., Lisanti,M.P., Baldini,G., Sargiacomo,M., Corley-Mastick,C. and Lodish,H.F. (1994) Induction of caveolin during adipogenesis and association of GLUT4 with caveolin-rich vesicles. *J. Cell Biol*., **127**, 1233–1243.

Scherer,P.E., Tang,Z.-L., Chun,M.C., Sargiacomo,M., Lodish,H.F. and Lisanti,M.P. (1995) Caveolin isoforms differ in their N-terminal protein sequence and subcellular distribution: identification and epitope mapping of an isoform-specific monoclonal antibody probe. *J. Biol. Chem*., **270**, 16395–16401.

Scherer,P.E., Okamoto,T., Chun,M., Nishimoto,I., Lodish,H.F. and Lisanti,M.P. (1996) Identification, sequence and expression of caveolin-2 defines a caveolin gene family. *Proc. Natl Acad. Sci. USA*, **93**, 131–135.

Scherer,P.E. *et al*. (1997) Cell-type and tissue-specific expression of caveolin-2. Caveolins 1 and 2 co-localize and form a stable hetero-oligomeric complex *in vivo*. *J. Biol. Chem*., **272**, 29337–29346.

Severs,N.J. (1988) Caveolae: static inpocketings of the plasma membrane, dynamic vesicles or plain artefact. *J. Cell Sci*., **90**, 341–348.

Shaul,P.W., Smart,E.J., Robinson,L.J., German,Z., Yuhanna,I.S., Ying,Y., Anderson,R.G.W. and Michel,T. (1996) Acylation targets endothelial nitric-oxide synthase to plasmalemmal caveolae. *J. Biol. Chem*., **271**, 6518–6522.

Shridhar,V., Sun,Q.C., Miller,O.J., Kalemkerian,G.P., Petros,J. and Smith,D.I. (1997) Loss of heterozygosity on the long arm of human chromosome 7 in sporadic renal cell carcinomas. *Oncogene*, **15**, 2727–2733.

Simionescu,N. and Simionsecu,M. (1983) The cardiovascular system. In Weiss,L. (ed.), *Histology: Cell and Tissue Biology.* Elsevier Biomedical, New York, NY, pp. 371–433.

Smart,E.J., Ying,Y., Mineo,C. and Anderson,R.G.W. (1995) A detergent free method for purifying caveolae membrane from tissue cultured cells. *Proc. Natl Acad. Sci. USA*, **92**, 10104–10108.

Song,K.S., Li,S., Okamoto,T., Quilliam,L., Sargiacomo,M. and Lisanti,M.P. (1996a) Copurification and direct interaction of Ras with caveolin, an integral membrane protein of caveolae microdomains. Detergent free purification of caveolae membranes. *J. Biol. Chem*., **271**, 9690–9697.

Song,K.S., Scherer,P.E., Tang,Z.-L., Okamoto,T., Li,S., Chafel,M., Chu,C., Kohtz,D.S. and Lisanti,M.P. (1996b) Expression of caveolin-3 in skeletal, cardiac and smooth muscle cells. Caveolin-3 is a component of the sarcolemma and co-fractionates with dystrophin and dystrophin-associated glycoproteins. *J. Biol. Chem.*, **271**, 15160–15165.

Tang,Z.-L., Scherer,P.E. and Lisanti,M.P. (1994) The primary sequence of murine caveolin reveals a conserved consensus site for phosphorylation by protein kinase C. *Gene*, **147**, 299–300.

Tang,Z.-L., Scherer,P.E., Okamoto,T., Song,K., Chu,C., Kohtz,D.S., Nishimoto,I., Lodish,H.F. and Lisanti,M.P. (1996) Molecular cloning of caveolin-3, a novel member of the caveolin gene family expressed predominantly in muscle. *J. Biol. Chem*., **271**, 2255–2261.

Wang,X.L., Uzawa,K., Miyakawa,A., Shiiba,M., Watanabe,T., Sato,T., Miya,T., Yokoe,H. and Tanzawa,H. (1998) Localization of a tumour-suppressor gene associated with human oral cancer on 7q31.1. *Int. J. Cancer*, **75**, 671–674.

Way,M. and Parton,R. (1995) M-caveolin, a muscle-specific caveolin-related protein. *FEBS Lett.*, **376**, 108–112.

Zenklusen,J.C., Rodriguez,L.V., LaCava,M., Wang,Z., Goldstein,L.S. and Conti,C.J. (1996).Novel susceptibility locus for mouse hepatomas: evidence for a conserved tumor suppressor gene. *Genome Res.*, **6**, 1070–1076.

Zenklusen,J.C., Hodges,L.C. and Conti,C.J. (1997) Loss of heterozygosity on murine chromosome 6 in two-stage carcinogenesis: evidence for a conserved tumor suppressor gene. *Oncogene*, **14**, 109–114.

Received May 13, 1998; revised August 17, 1998; accepted September 14, 1998

Note added in proof

While this work was under review, a paper appeared showing that disruption of caveolae by cholesterol depletion (using the cholesterol binding agent cyclodextrin) is sufficient to hyperactivate ERK (Furuchi *et al*., 1998). Thus, disruption of caveolae formation by either cholesterol depletion (Furuchi *et al*., 1998) or caveolin-1 depletion (this report) constitutively activates the p42/44 MAP kinase cascade. As such, these cholesterol depletion studies directly support our current observations made using an anti-sense approach.